Journal of Ceramic Processing Research. Vol. 15, No. 2, pp. 66~70 (2014)

J O U R N A L O F
Ceramic Processing Research

Trench-filling behavior of Ge-Sb chalcogenide films prepared by various atomic vapor deposition

Hyung Keun Kim, Jin Hwan Jeong, Su Bin An and Doo Jin Choi*
Department of Materials Science and Engineering, Yonsei University, 262 Seong Sanno, Seodaemun-gu, Seoul 120-749, Korea

Ge-Sb phase-change film was deposited into a trenched structure with trenches 40 nm in diameter by means of atomic vapor deposition, and the trench-covering ability of the film was determined under various conditions. Three different plasma conditions were created in the reaction chamber-non-plasma, semi-shielded plasma, and direct plasma-by inserting or removing a metal grid in the middle of the reaction chamber. In addition, film composition was varied among Ge, Ge-Sb, and Sb. Partial pressure and time of flight of precursor molecules in the reaction chamber were varied by controlling precursor feeding time and precursor injection position, respectively. The origin of the trench-covering ability of the films was analyzed by applying the concept of an effective sticking coefficient.

Key words: Phase change materials, Trench-covering ability, Atomic vapor deposition, Multi-scale modeling, Effective sticking coefficient.

Introduction

There are critical issues related to operational power consumption of next-generation non-volatile memory devices. Many attempts have been made to solve these issues, including the strategy of using phase-change random access memory by increasing electrical resistance of the crystalline phase of a phase-change material [1-3]. A novel cell structure, called a trench-structured cell or confined cell, has been studied extensively in this context. It is advantageous to minimize thermal energy loss and thermal cross talk among adjacent memory cells during the phase transition process, because the heating point in phase change materials is located inside the dielectric material [4]. It is well known that to deposit a phase change film into a trenched structure, chemical vapor deposition (CVD) or a similar film deposition process should be applied rather than conventional physical vapor deposition (PVD) [5], because conventional PVD methods (especially sputtering) do not provide adequate step coverage [5, 6]. In our previous report, we described Ge-Sb phase-change film prepared by plasma-enhanced atomic vapor deposition (AVD) [6]. However, the trench covering ability (TCA) of films is rarely reported despite many reports of chemical vapor deposition (CVD) of phase-change films [6-8]. We extend our previous research in this paper by describing the TCA of Ge-Sb phase-change films deposited by AVD into a trenched structure with a trench diameter of 40 nm, which is to our knowledge one of the narrowest trenches reported. We also consider the dependency of TCA on the plasma ignition conditions used, film composition, and the partial pressure of gaseous precursor molecules in the reaction chamber and near the substrate surface. In addition, we perform a theoretical analysis of the origin of trench-covering ability.

*Corresponding author:
Tel : +82-2-2123-2852
Fax: +82-2-312-5375
E-mail: drchoidj@yonsei.ac.kr

Experimental Details

Trench structures with a trench diameter of 40 nm and depth of 100 nm were etched on Si_3N_4 (100 nm)/p-type Si(100) wafer surfaces, as depicted in Fig. 1a. Then, GeSb phase-change films were deposited onto these substrates at the deposition temperature of 200 °C using an AVD system. This multi-channel AVD system employed direct liquid delivery using a pulsed spray evaporator, and was fully customized for fine control of film deposition. Tetra(isobutyl)germanium (TiBGe) and tri(isopropyl)antimony (TiPSb) were selected as the precursors of Ge and Sb, respectively. Ar and H_2 gases, used as the precursor carrier gas and reactant gas, respectively, were continuously flowed into the reaction chamber to maintain the pressure at 3 Torr. A schematic diagram of the reaction chamber is provided in Fig. 1b. Plasma with a power of 60 W was ignited in a quartz tube attached to the reaction chamber. Three different plasma conditions were studied; these conditions were created by inserting or removing a metal grid in the middle of the reaction chamber. According to the three different plasma conditions, three AVD processes were used: thermal AVD (THMAVD) without plasma ignition; semi-shielded plasma-enhanced AVD with the metal grid in place (SPEAVD) to reduce ion bombardment;

and plasma-enhanced AVD with direct plasma exposure (DPEAVD) with the metal grid removed. We also varied the partial pressure of the gaseous precursor molecules in the THMAVD process by varying the precursor feeding time between 0.5 and 2.0 s. In addition, the precursor injection position was varied between the top and bottom sides of the reaction chamber. Cross-sectional images of trenched structures containing phase-change films were taken by scanning electron microscopy and field-effect scanning electron microscopy (SEM and FESEM, JEOL JSM-7001F) as well as transmission electron microscopy (TEM, JEOL JEM-2100). For TEM observations, specimens were fabricated by the focused ion beam method.

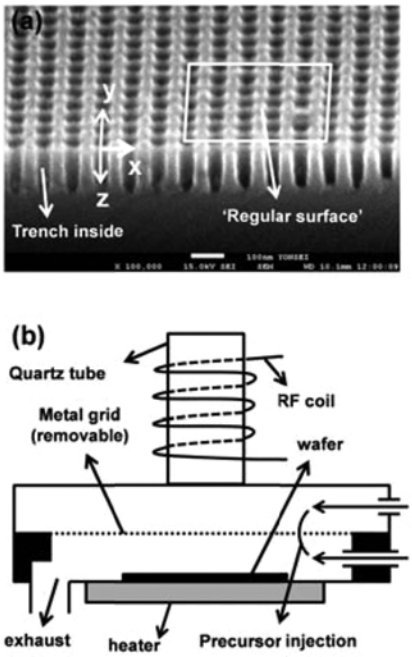

Fig. 1. (a) Cross-sectional SEM image of a trench-structured wafer with a trench diameter of 40 nm and trench depth of 100 nm; (b) schematic diagram of the reaction chamber.

Results and Discussion

TCA was determined for the three plasma conditions and three film compositions, as depicted in Fig. 2. Ge-Sb refers to the binary composition that results from a 1 : 3 feeding cycle ratio of Ge and Sb precursors; namely, $Ge_{0.38}Sb_{0.62}$, as detailed in our previous report [6]. The TCAs of all specimens in the case of THMAVD were quite good (Figs. 2a, 2d, and 2 g). In the case of SPEAVD, the TCAs of Ge and GeSb were also good, while surface agglomerations of GeSb and Sb film at the regular surface were increased relative to THMAVD. In the case of DPEAVD, only the Ge film showed a high TCA, while no trench covering was evident when GeSb or Sb film was applied; additionally, GeSb and Sb films showed greater agglomeration at the regular surface. To understand the differences in TCA according to conditions by modeling, we used multi-scale modeling, a methodology often used to simulate CVD [9-12]. Use of multi-scale modeling was necessitated by the considerable difference in scale between the CVD chamber (300 mm wide and 150 mm

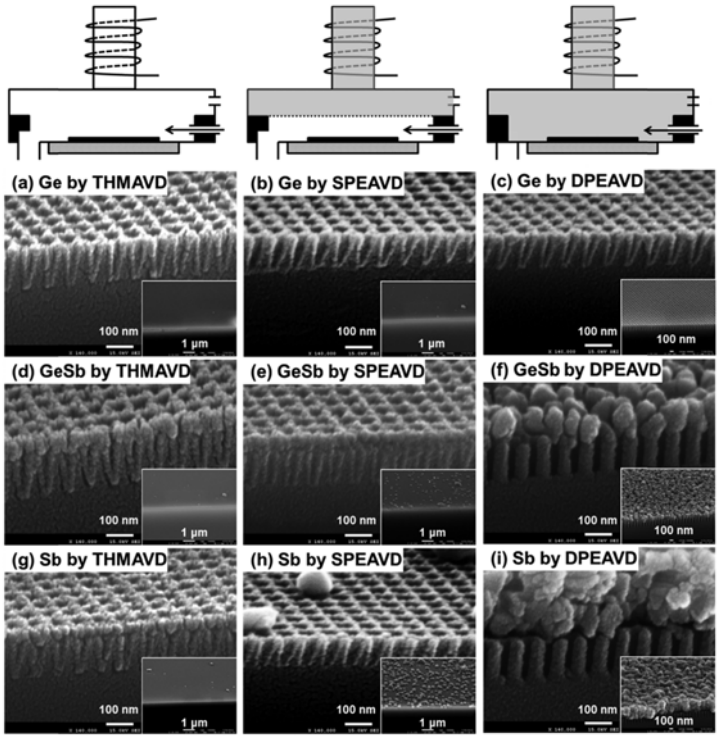

Fig. 2. Cross-sectional SEM image of the (a-c) Ge, (d-f) GeSb and (g-i) Sb deposited films on the trench structure substrate in each condition using thermal AVD (THMAVD), semi-shielded plasma-enhanced AVD (SPEAVD), and direct plasma-enhanced AVD (DPEAVD).

Table 1. Calculated MFP and Knudsen numbers of TiBGe and TiPSb in the chamber and trench regions.

Molecule diameter (m)		MFP (m)	Kn	
			Chamber (D_H 8.99×10^{-2} m)	Trench (D_H 40×10^{-9} m)
TiBGe	5.26×10^{-10}	1.33×10^{-5}	1.48×10^{-4}	332.5
TiPSb	4.14×10^{-10}	2.15×10^{-5}	2.39×10^{-4}	537.5

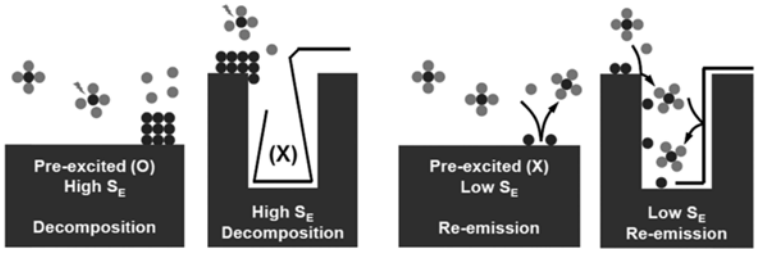

Fig. 3. Schematics of film deposition for (a) high and (b) low sticking coefficients.

tall) and the trench cell (40 nm wide and 100 nm deep in our experiments); because of the different mechanisms of flow and deposition of gaseous precursor molecules in these extremely different environments, an understanding is needed of the relationship between the chamber scale and the trench scale. Cheimarios and colleagues reported that the behaviors of gaseous precursor molecules could be clarified at the reactor scale (chamber scale), feature scale (trench scale), and nano-morphological scale (atomic scale on the substrate surface) by applying different simulation methodologies for each scale [9, 10]; TCA was one of the deposition parameters reported in these studies. For gaseous molecules traveling in a large-scale reaction chamber (reactor scale), a viscous fluent model can be used to simulate their motions; however, within a trench structure, a ballistic model should be used. In general, the criteria used in a multi-scale model are the mean free path (MFP) of the gaseous precursor molecules and the size of the deposition system, which is expressed as the Knudsen number (K_n). as shown in the equations below [13]:

$$\lambda = \frac{\kappa_B T}{\sqrt{2\pi d^2 P}}$$

$$K_n = \frac{\lambda}{D_H}$$

Here, λ refers to the MFP and D_H indicates the spatial size of the deposition system. The diameter of each precursor was calculated based on its atomic radius in a covalent bond (Ge = 1.25×10^{-10} m, Sb = 1.45×10^{-10} m, C = 7.00×10^{-11} m, H = 2.50×10^{-11} m). MFPs and K_n were calculated for our experimental environments; these data are shown in Table 1. The gas flow mechanism is known to differ in relation to K_n [13, 14]; when K_n is smaller than 0.01, the system is 100 times larger than the MFP and the flow of gaseous molecules proceeds through a viscous flow mechanism. When K_n is between 0.01 and 1, the relevant system is slightly larger than the MFP; within this range, the flow mechanism transitions from viscous flow to molecular flow. When K_n is larger than 1, the MFP is considerably longer than the dimensions of the system and flow proceeds through a molecular flow mechanism. In our experiments, we modeled gas flow in the chamber using a viscous fluent model, while we modeled gas flow in trenches or nearby regular surfaces using a molecular flow mechanism (ballistic model) [9]. Deposition of precursors inside the trench structure can be explained by the concept of the local effective sticking coefficient (S_E), as shown in the following equation [10]:

$$S_{E,i}(\mathrm{x}) = \frac{\gamma_i r^s N_A}{\Gamma_i(\mathrm{x})}$$

The effective sticking coefficient $S_{E,i}$ of component i at position x is proportional to the surface energy (γ_i) of component i to the substrate surface and the reactivity r. In addition, $S_{E,i}$ is inversely proportional to the flux [$\Gamma_i(x)$] of component i at position x. The aspects of precursor deposition and trench covering are depicted in Fig. 3. S_E decreases and the probability of re-emission increases as the reactivity of the precursor molecules decreases and as the flux of their collisions with the substrate surface increases. These re-emissions increase the number of precursor molecules that are inserted into the trenched structure, thereby increasing the overall TCA. We found that gaseous precursor molecules were most excited (and thus S_E was highest and TCA was the worst) under the plasma conditions of DPEAVD, followed by SPEAVD, and then by THMAVD; that is, the THMAVD process yielded the best TCA due to its lower excitation of gaseous precursors (Fig. 2). TCA was clearly reduced under plasma conditions (Figs. 2g-i). While the trench

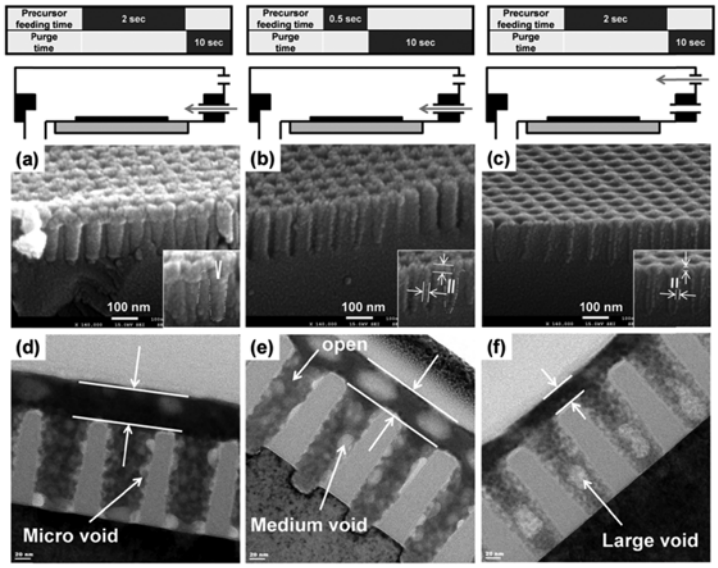

Fig. 4. Images taken by (a-c) SEM and (d-f) TEM showing TCA for each condition.

structure was covered quite well by THMAVD, TCA decreased gradually in response to plasma AVD. Finally, trenches were isolated with overhangs due to the high reactivity of the pre-excited precursor. This plasma effect also manifested as increased agglomeration on the regular surface upon excitation of the precursor (see Figure 2 insets). This surface agglomeration is thought to be related to the metallic property of Sb. That is, metallic Sb nuclei coalesce with other nuclei rather than spreading out to form a film on hydrophilic surfaces like Si_3N_4 [15]. Therefore, surface agglomeration increases with increasing Sb content, resulting in a granular surface morphology. Increased agglomeration at the regular surface with increasing Sb composition is clearly shown in Figs. 2b, 2e, and 2 h.

The precursor feeding time per cycle was set to 2.0 or 0.5 s with a fixed purge time of 10 s to analyze changes in TCA with respect to the partial pressure of the precursor molecules in the reaction chamber. The inside of the trench structure was completely filled when using a feeding time of 2 s, while it was incompletely filled when using a feeding time of 0.5 s, despite film deposition on the regular surface with a thickness of 40 nm (Figs. 4a-b). Transmission electron microscopy was performed to more clearly observe the TCA; it revealed that both the size and number of voids in the trenches after 0.5 s of feeding were greater than those after 2 s of feeding, and film was deposited on the regular surface, while the entrance of the trenches were open (Figs. 4d-e). This is thought to occur because the partial pressure of the precursor in the reaction chamber affects S_E. At a high partial pressure, the number of precursor molecules colliding with the unit substrate surface area during a unit of time increases. This means that a high partial pressure increases the flux of precursor molecules colliding with the substrate surface and decreases S_E. Finally, the decreased S_E enhances TCA, as explained above.

TCA changes according to precursor injection position are shown in Figs. 4a and 4c. In these figures, there were no clear differences in TCA; only the difference in film thickness was obvious. However, TCA changes were observed clearly by TEM. When the precursor was injected at the top side (near the roof of the chamber), large voids formed in the middle of the trenches, as shown in Fig. 4f. When precursor was injected in the bottom side (directly above the substrate), only micro-voids formed without any large voids, as shown in Fig. 4d. These results are due to differences in time of flight and local partial pressure near the substrate surface according to precursor injection position. With respect to time of flight, S_E increased and TCA decreased, as shown in Figs. 4c and 4f, because the probability of being pre-excited increases with increased time of flight. With respect to local partial pressure, S_E increased due to the low flux of precursor molecules colliding with the substrate surface, because local partial pressures near the substrate surface were low due to the greater distance from the precursor injection position to the substrate surface.

Conclusions

GeSb phase-change films were deposited in trenched structures, and their TCA was analyzed based on our previous report concerning the phase transition characteristics and film deposition behavior of an AVD system. To understand the parameters of film deposition and to control the TCA of precursors, we performed multi-scale modeling of gaseous molecule flow to design the experiments. We calculated the MFP

and K_n of each precursor at both the chamber scale and the trench scale, and found that flow within the trench structure was best modeled using a ballistic molecular flow mechanism. TCA and film deposition behavior changed according to deposition parameters such as plasma conditions, film composition, precursor feeding time, and precursor injection position. We related the observed changes in TCA and film deposition to deposition parameters using the concept of an effective sticking coefficient, which is affected by pre-excitation and flux of precursor molecules as well as interactions between the films and hydrophilic surfaces. We found that real deposition behavior inside very small trench structures matched well with predicted behavior based on theoretical considerations.

References

1. H. K. Kim, N. H. Kim, D. J. Choi, J. mater. Sci. 47 (2012) 6679.
2. H. K. Kim, J. S. Roh, D. J. Choi, Thin Solid Films 518 (2010) 6422.
3. B. Qiao, Q. Guo, A. G. Tian, G. L. Pan, L. B. Xu, J. Electron. Mater. 36 (2007) 88.
4. G. W. Burr, M. J. Breitwisch, M. Franceschini, D. Garetto, K. Gopalakrishnan, B. Jackson, B. Kurdi, C. Lam, L. A. Lastras, A. Padilla, B. Rajendran, S. Raoux, R. S. Shenoy, J. Vac. Sci. Technol. B 28 (2010) 223.
5. J. I. Lee, H. Park, S. L. Choi, Y. L. Park, B. J. Bae, J. H. Park, J. S. Park, H. G. An, J. S. Bae, D. H. Ahn, Y. T. Kim, H. Horii, S. A. Song, J. C. Shin, S. O. Park, H. S. Kim, U-in. Chung, J. T. Moon, B. -I. Ryu, 2007 IEEE Symposium on VLSI Technology (2007) 102.
6. H. K. Kim, J. H. Jung, D. J. Choi, Thin Solid Films 520 (2012) 6947.
7. M. Longo, O. Salicio, C. Wiemer, R. Fallica, A. Molle, M. Fanciulli, C. Giesen, B. Seitzinger, P. K. Baumann, M. Heuken, S. Rushworth, J. Cryst. Growth 310 (2008) 5053.
8. D. Reso, M. Silinskas, M. Lisker, A. Gewalt, E. P. Burte, Thin Solid Films 529 (2011) 2150.
9. N. Cheimarios, S. Garnelis, G. Kokkoris, A. G. Boudouvis, J. Nanosci. Nanotechno. 11 (2011) 8132.
10. N. Cheimarios, G. Kokkoris, A. G. Boudouvis, Chem. Eng. Sci. 65 (2010) 5018.
11. S. T. Rodgers, K. F. Jensen, J. Appl. Phys. 83 (1998) 524.
12. T. P. Merchant, M. K. Gobbert, T. S. Cale, L. J. Borucki, Thin Solid Films 365 (2000) 368.
13. M. Ohring, Materials Science of Thin Films, Academic Press, San Diego (2002).
14. M. K. Gobbert, T. S. Cale, J. Comput. Phys. 213 (2006) 591.
15. Z. Li, A. Rahtu, R. G. Gordon, J. Electrochem. Soc. 153 (2006) C787.